CONF-950518--12
ANL/CHM/CP-86550

HIGH RESOLUTION TRANSMISSION ELECTRON MICROSCOPY STUDY OF DIAMOND FILMS GROWN FROM FULLERENE PRECURSORS*

J. S. Luo, D. M. Gruen, A. R. Krauss
Chemical Technology, Materials Science, and Chemistry Divisions
Argonne National Laboratory
Argonne, Illinois 60439

X. Z. Pan
Physics Department, Wuhan University
Wuhan Hubei 430072, China

and

S. Z. Liu
QQC, Inc.
Dearborn, Michigan 48126

Submitted for the Proceedings of the

Symposium on "The Fullerenes: Chemistry, Physics, and New Directions"
187th Meeting of the Electrochemical Society

Reno, Nevada,

May 21-26, 1995

*Work supported by the U.S. Department of Energy, BES-Material Sciences, under Contract W-31-109-ENG-38.

DISCLAIMER

DISCLAIMER

Portions of this document may be illegible in electronic image products. Images are produced from the best available original document.

High Resolution Transmission Electron Microscopy Study of Diamond Films Grown from Fullerene Precursors

J. S. Luo[1], D. M. Gruen[1], A. R. Krauss[1], X. Z. Pan[1], and S. Z. Liu[2]
[1]Argonne National Laboratory, Argonne, IL 60439
[2]QQC, Inc., Dearborn, MI 48126

Abstract

High-resolution transmission electron microscopy (HRTEM) has been used to investigate the microstructure of diamond films grown by plasma-assisted chemical vapor deposition using fullerene precursors. HRTEM observations of as-grown films revealed an array of larger crystals (>200 nm) within a polycrystalline matrix of much smaller crystallites (<20 nm). The randomly oriented small crystallites were nearly free of structural imperfections such as stacking faults or twins, while the larger ones had preferred <110> orientations with respect to the Si (100) substrate and showed evidence of structural defects on the periphery of the crystals. The most common defects were V-shaped $\Sigma 9$ twin boundaries, which are generally believed to serve as re-entrant sites for diamond nucleation and growth. The observation of growth steps on both {111} and {110} surfaces seems to support a reaction model in which fragments of C_{60}, including C_2, are considered the growth species. In particular, the nanocrystallinity of the films is most likely due to a high carbon cluster density from C_{60} fragmentation at or near the diamond surface, which can serve as nucleation sites for the growth of new crystallites.

Numerous efforts have been made to grow high-quality diamond films by chemical vapor deposition (CVD). Such films are potentially useful for a wide range of applications because of diamond's outstanding physico-chemical properties, such as hardness, thermal conductivity, chemical and thermal stability, electrical resistance, hole and electron mobilities, and optical transparency.[1,2] In general, growth of diamond films by CVD involves a competitive process of nucleation and growth among various forms of carbon (diamond, graphite, or amorphous carbon) and requires precise control of processing parameters and precursor constituents.[2-4] Bachmann *et al.*[5] reported, based on the gas compositions used experimentally to grow diamond films in the past 30 years, that the formation domain for the diamond phase is compositionally quite narrowly defined within a triangular portion of a C-H-O diagram. It is generally believed that a large excess of hydrogen (up to 99% of the gas phase) is indispensable for the nucleation and growth of the diamond phase, even though the exact role of hydrogen in the growth mechanism has not been fully clarified.[2-4] The effect of the types of carbon precursor used on diamond film growth has also been much discussed.[6]

Recently, Gruen *et al.*[7,8] reported that nano-crystalline diamond films were grown by using fullerene precursors in an argon microwave plasma. The authors suggested that the collisional fragmentation of C_{60} into reactive carbon species, such as C_2, is likely responsible for the diamond growth under these conditions. The purpose of the present work is to investigate the mechanisms of diamond nucleation and growth from fullerene precursors by using high resolution transmission electron microscopy (HRTEM) to examine the microstructural and crystallographic

features and structural defects of the diamond crystals produced by this method.

The diamond films were grown in a modified ASTeX microwave plasma chamber. The experimental details have been described elsewhere.[7] In brief, fullerene-containing soot was degassed, treated with methanol to remove hydrocarbon, and placed in a sublimator located in a sidearm of the plasma chamber. Fullerene vapor was then introduced into the plasma chamber by heating the sublimator to 550°C while flowing argon carrier gas through it. The atomic carbon content of the carrier gas was estimated to be about 0.14% based on the vapor pressure of pure C_{60}.[7,8] Deposition was carried out at 850°C with 1500 W of microwave power for 3 hours on a silicon (100) substrate that had been polished with diamond powder. Plan-view specimens for HRTEM studies were prepared by chemically removing the silicon substrate and subsequently ion milling the film. The HRTEM observations were carried out by using a JEOL 4000 EX microscope with a point-to-point resolution of 0.16 nm at 400 kV with a biaxial tilt of 20°.

Figure 1 shows a typical area of an as-deposited film consisting of an array of larger crystals (~300 nm) within a polycrystalline matrix of much smaller crystallites (<20 nm). The inset electron diffraction pattern indicates fine polycrystallites of cubic diamond. The larger crystals tend to have <110> orientation, while smaller ones appear to have random orientation with respect to the Si (100) substrate. Many of the diamond crystallites showed well-developed facets (see arrows in Fig. 1), which correspond to low-index faces of diamond.[9] The common crystalline surfaces were of the {111} or {100} type, so the crystal morphology was either octahedral or cuboctahedral.[10] In addition, {110}-type surfaces

were observed, which typically showed triangular forms in HRTEM (see double arrows in Fig. 1). The average grain size of the as-grown diamond crystallites was about two orders of magnitude smaller than that of diamond film grown using a standard H_2-CH_4-O_2 gas mixture, indicating a much higher nucleation density.[11] Meilunas *et al.*[12] reported an enhancement in diamond nucleation density when C_{70} was deposited on a Si (100) surface, with subsequent diamond film growth in a H_2-CH_4-O_2 plasma. They also found that seeding with C_{60} did not result in enhanced nucleation density. The enhancement observed for C_{70} compared with C_{60} films was rationalized in terms of a better match between the carbon atom arrangement in the C_{70} molecule (which has chair-form cyclohexane linkages) and the diamond {111} surface. It is postulated in the present work that the degree of fragmentation resulting from the interaction of the precursor with the argon plasma is sufficient to eliminate significant differences between C_{60} and C_{70} precursors.[13] This point has practical significance since C_{70} is only a minor component of the fullerene soot, and the cost of the carbon source material is influenced by both the abundance of the selected fullerene species and the cost of extracting it. We have been able to use raw soot without extraction, relying on the relatively high vapor pressure of C_{60} to produce a highly phase-pure C_{60} vapor.[7,8]

Figure 2 shows a typical polygonized diamond crystallite viewed along its [111] direction, i.e., roughly normal to the Si (100) substrate. The crystallite had well-developed facets corresponding to {110} surfaces of cubic diamond, as determined by electron diffraction and measured lattice spacings. These surfaces seemed rather smooth, with evidence of lateral growth (along the direction parallel to the Si (100) substrate surface), indicating a layer-by-layer growth mechanism (see the arrow in Fig. 2).

The inset image shows an enlargement of the edge area where growth steps on a (110) surface were clearly observed. This result is consistent with the general belief that diamond crystallites undergo layer-by-layer growth after they have developed faceting.[10] It is also interesting to note that this diamond crystallite was nearly free of structural imperfections, judging from the uniform appearance of its lattice images over the entire area, except for a few regions close to the edges. Reduction of structural defects in CVD diamond films has important implications, because defect-free diamond films exhibit much superior physical properties.[1,10] Our results indicate that the use of fullerene precursors appears to be responsible for the growth of nearly perfect diamond crystallites in a large volume fraction. By comparison, diamond films grown from the conventional CH_4-H_2-O_2 gas mixtures contained a large number of stacking faults and twins lying on {111} planes.[11,14]

Interestingly, nearly all the small diamond crystallites (<20 nm) observed appeared faultless. One such crystallite is shown in Fig. 3a. This elongated crystallite was viewed roughly along its [110] direction so that the (111) lattice planes ($d_{(111)}$ = ~0.20 nm) could be measured (see Figs. 3b and 3c for enlarged views). The (111) lattice fringes were uniform over the entire crystallite, and there was no evidence of stacking faults or microtwins on the (111) surface. Growth steps were also observed on the (111) surface, as shown in Fig. 3b, indicating a layer growth mechanism. An apparent disordered phase, which showed an amorphous type contrast, was observed at the growth front of the diamond (111) surface (see enlarged images of areas 3b and 3c). By shifting the microscope plane of focus slightly, the underlying diamond structure could be seen, indicating that the amorphous region is no more than a few nanometers thick.

Another interesting feature observed in this crystallite was secondary nucleation on the (111) surface (see Fig. 3c). In this case, the <10 nm size nucleus was not necessarily epitaxial with respect to its matrix crystallite, as could be seen from the difference in orientation of (111) lattice fringes between the matrix crystallite and the nucleus (see Fig. 3c). Such a secondary nucleation mechanism could be the cause of the high nucleation rate observed in this film, which in turn could lead to nano-sized diamond grains.

The larger diamond crystals (typically around 300 nm) had preferred <110>-type orientation with respect to the Si (100) substrate. These crystals did not have well-defined outlines and developed structural defects on the peripheries (see Fig. 4). Many of these defects had a "V" shape with an angle of ~70° between two edges, characteristic of $\Sigma 9$ twin boundaries in CVD diamond films (see arrows in Fig. 4).[15] The $\Sigma 9$ boundary forms on a surface that is the locus of intersection points of growing planes on two adjacent crystals; therefore, it indicates the local growth directions.[15] It can be seen from the enlarged inset image that the local growth appeared to be on the adjacent {111} planes, occurring through a layer-by-layer growth mechanism along a well-defined <112> direction. It is generally believed that V-shaped $\Sigma 9$ twin boundaries serve as re-entrant sites for the rapid growth of the diamond phase, because the carbon atoms are more stable in these sites, which are located at propagating {111} planes.

In summary, HRTEM has been used to investigate the microstructure of diamond films grown from a fullerene precursor. The films were comprised nearly entirely of an array of larger crystals within a polycrystalline matrix of much smaller crystallites. The small

crystallites, having a typical size of <20 nm, were randomly oriented with respect to the Si (100) substrate and were nearly free of structural imperfections. The larger crystallites had preferred <110>-type orientation with respect to the Si (100) substrate and developed structural defects on the periphery of the crystals. The most common defects were V-shaped $\Sigma 9$ twin boundaries, which are the re-entrant sites for fast diamond growth. Growth was observed to occur primarily on {111} and {110} surfaces, apparently by a layer-by-layer growth mechanism. The high nucleation rates observed in as-grown films were likely caused by secondary nucleation on {111}-type surfaces. As Angus and Hayman[3] have pointed out, the atomic structure of diamond surfaces directs precursor adatoms to specific sites to accommodate the different types of vacant surface sites available on the planes. Therefore, carbon dimer species are thought to be preferred by {110} surfaces,[3,16] while compounds with either cyclocarbon linkages or carbon dimers can be incorporated on {111} surfaces.[3,7,12] Indeed, optical spectroscopy showed abundant C_2 molecules in the plasma, as a result of the fragmentation of C_{60} by collisionally and/or thermally induced dissociation processes.[7,8] There is also evidence that carbon clusters larger than C_2 are present in the plasma as a result of incomplete fragmentation processes.[7,13] Consequently, our HRTEM observation of growth steps on both {110} and {111} surfaces seems to support a growth model proposed by Gruen *et al.*[7,8], in which fragments of C_{60}, including C_2,are considered the growth species. In particular, the nanocrystallinity of the films is most likely due to a high carbon cluster density from C_{60} fragmentation at or near the diamond surface, which can serve as nucleation sites for the growth of new crystallites.

ACKNOWLEDGMENT

The authors gratefully acknowledge Drs. R. Csencsits and N. Zaluzec for useful discussions, Dr. V. A. Maroni for his critical reading of the manuscript, and J. Andrew for editorial assistance. The work at Argonne National Laboratory was sponsored by the U.S. Department of Energy (DOE), BES-Materials Science, under Contract W-31-109-ENG-38.

REFERENCES

[1]J. E. Field, *Properties of Diamond*, Academic Press, London, 1979.

[2]W. A. Yarbrough, J. Am. Ceram. Soc. **75**, 3179 (1992).

[3]J. C. Angus and C. C. Hayman, Science **241**, 913 (1988).

[4]W. A. Yarbrough and R. Messier, Science **247**, 688 (1990).

[5]P. K. Bachmann, D. Leers, and H. Lydtin, Diamond and Related Materials **1**, 1 (1991).

[6]J. C. Angus, R. W. Hoffman, and P. H. Schmidt, *Science and Technology of New Diamond*, KTK Terra Scientific, Tokyo, 1990.

[7]D. M. Gruen, S. Liu, A. R. Krauss, and X. Pan, J. Appl. Phys **75**, 1758 (1994).

[8]D. M. Gruen, S. Liu, A. R. Krauss, J. S. Luo, and X. Pan, Appl. Phys. Lett. **64**, 1502 (1994).

[9]S. Iijima, Y. Aikawa, and K. Baba, J. Mater. Res. **6**, 1491 (1991).

[10]W. Zhu, B. R. Stone, B. E. Williams, and J. Y. Glass, Proceedings of the IEEE **79**, 621 (1991).

[11]D. M. Gruen, X. Pan, A. R. Krauss, S. Liu, J. S. Luo, and C. M. Foster, J. Vac. Sci. Technol. **A12**, 1491 (1994).

[12]R. Meilunas, R. P. H. Chang, S. Liu, and M. M. Kappes, Appl. Phys. Lett. **59**, 3461 (1991).

[13]D. M. Gruen, Nucl. Instrum. Methods, Phys. Res. B **78**, 118 (1993).

[14]B. E. William and J. T. Glass, J. Mater. Res. **4**, 373 (1989).

[15]D. Shechtman, J. L. Hutchison, L. H. Robins, E. N. Farabaugh, and A. Feldman, J. Mater. Res. **8**, 473 (1993).

[16]D. N. Belton and S. J. Harris, J. Chem. Phys. **96**, 2371(1992)

Figure Captions

Figure 1. Plan-view electron micrograph of the diamond film grown from fullerene precursors. Arrows indicate faceted diamond crystallites. The inset diffraction pattern can be indexed to an face-centered cubic diamond structure, and the systematic absences of {200} and {211} reflections are consistent with the space group (*Fd3m*).

Figure 2. Electron micrograph showing a diamond crystallite faceted with a (110) surface. The growth steps on the (110) surface are shown in the inset image.

Figure 3. Electron micrographs of (a) the morphology of a faultless diamond crystallite, (b) growth steps on the (111) surface, and (c) secondary nucleation on the (111) surface.

Figure 4. Electron micrograph of a well-grown diamond crystallite showing V-shaped $\Sigma 9$ boundaries on the periphery. Inset image indicates a local growth on the adjacent {111} planes along <112> directions.


140 nm

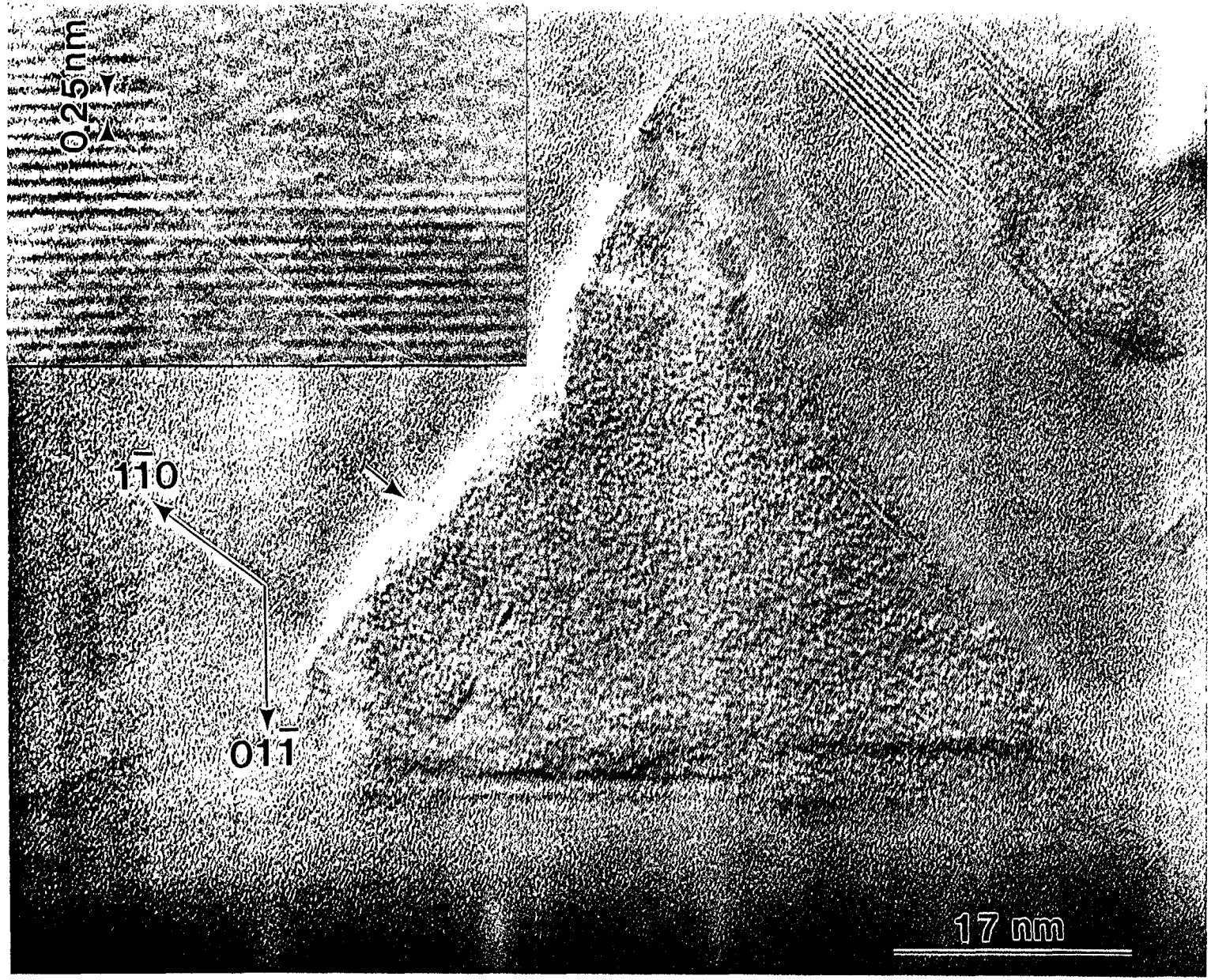
0.25 nm
$\bar{1}10$
$01\bar{1}$
17 nm

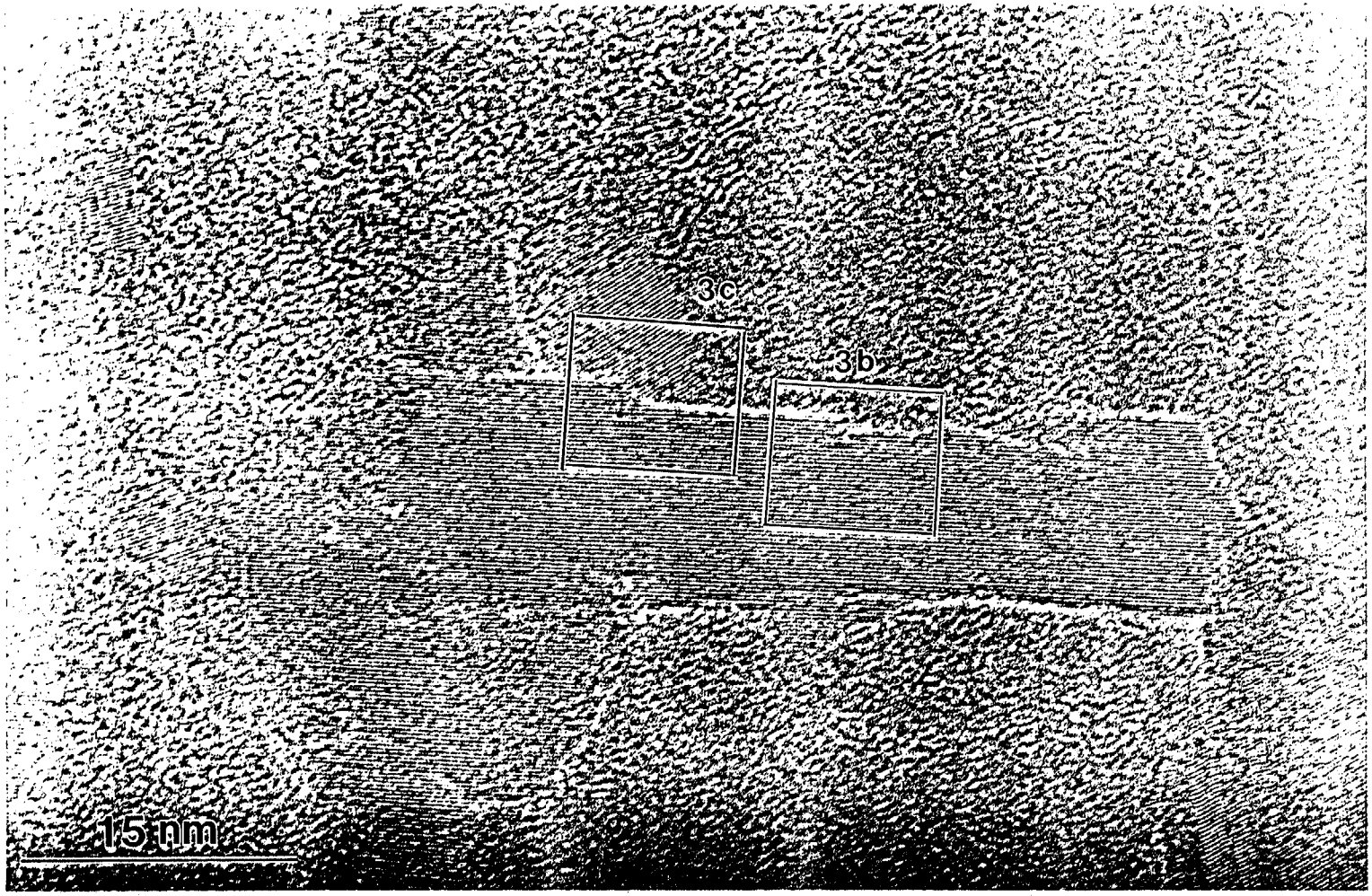
3c
3b
15 nm

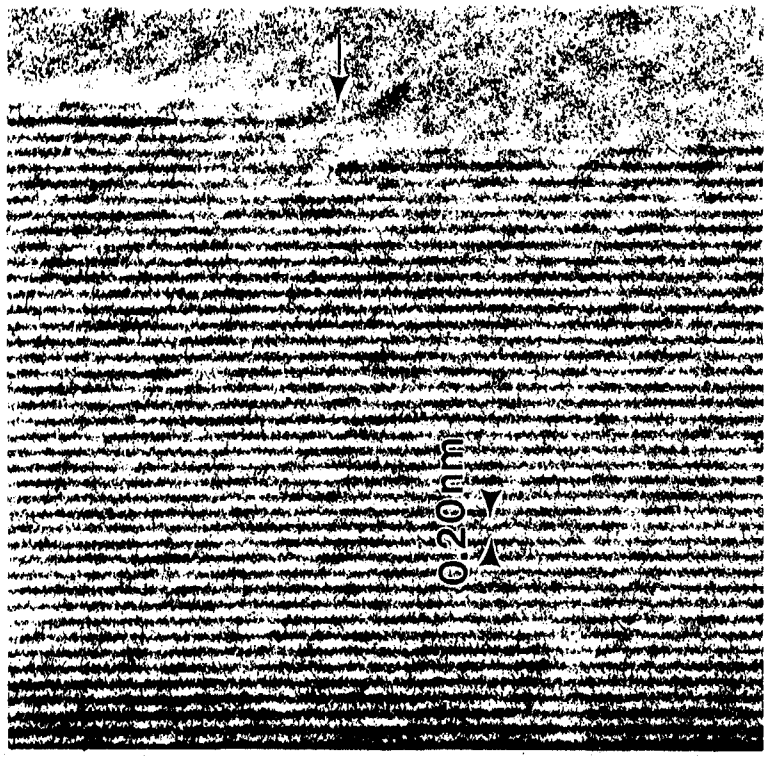

3b

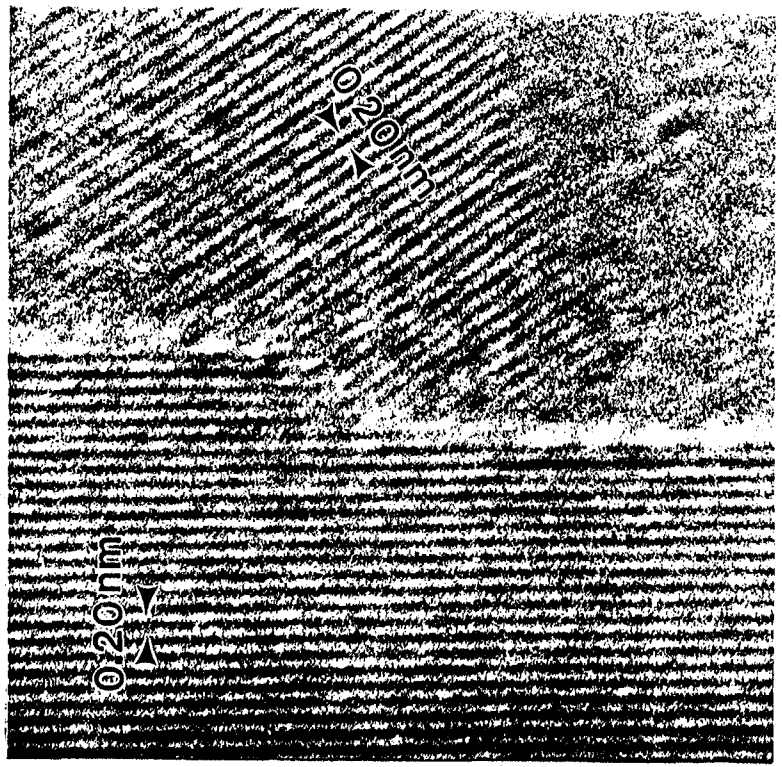

3c

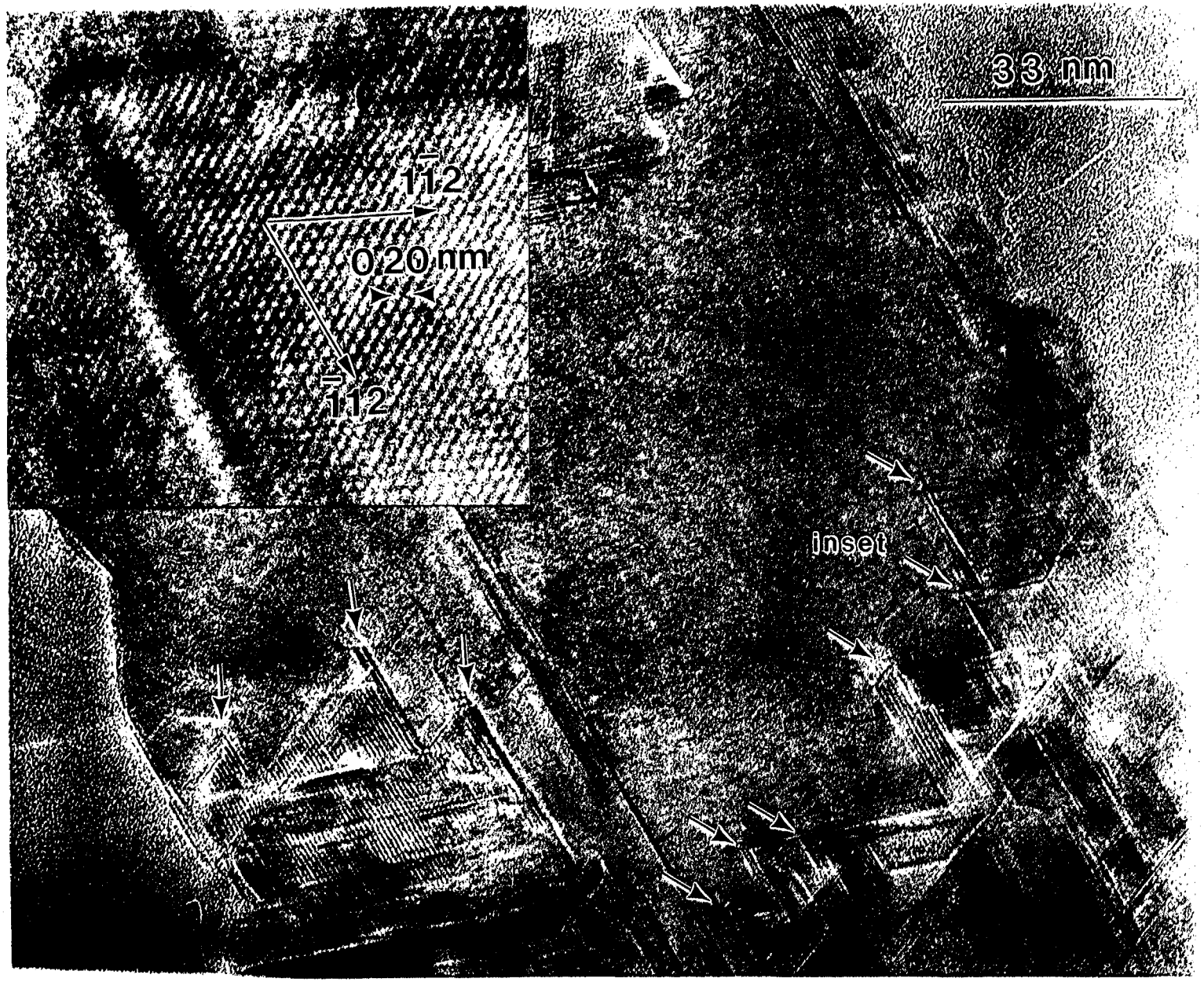
33 nm
$\bar{1}12$
0.20 nm
$\bar{1}12$
inset